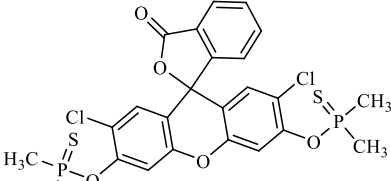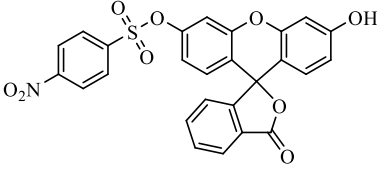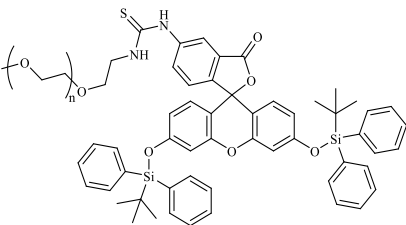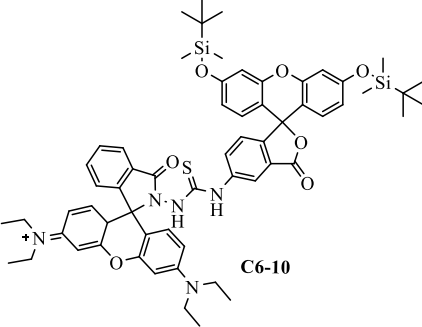Chapter 6

Detection of Fluoride in water with Fluorescein Dye-A Colorimetric and Fluorometric

6.1. Introduction

Fluorescein, discovered by Adolf von Baeyer in 1871, is well-known for its bright fluorescence, which is sensitive to variations in environmental factors like solvent polarity and pH [1,2]. Fluorescein has become essential in various scientific and medical research areas owing to its exceptional photophysical characteristics [3]. Fluorescein is extensively utilized as fluorescent probes and labels due to its high extinction coefficient, emission intensity, and quantum yields in aqueous solutions [4]. The chemical structure of the compound, which features a xanthene core fused with a benzene ring along with hydroxyl and carboxyl groups, provides remarkable versatility and reactivity. This enables its modification and conjugation with various biomolecules and substrates for a wide range of specific applications. These unique properties have rendered fluorescein derivatives indispensable as fluorescent tracers and dyes, significantly advancing biological research, medical diagnostics, environmental monitoring, and analytical chemistry. Upon excitation with light, typically in the blue region (around 490 nm), fluorescein emits a bright green fluorescence (around 520 nm) [4,5]. Fluorescein is also highly photostable, making fluorescein a reliable marker in long-term imaging and monitoring experiments. The high quantum yield of fluorescein is also enhancing its detection sensitivity, making it a suitable reporter unit for chemosensor development. Furthermore, the fluorescence of fluorescein is highly sensitive to pH, exhibiting strong fluorescence in neutral to slightly basic conditions (pH 6-9), which can be exploited in various pH-sensitive assays and applications. By appropriate modification in its chemical structure, researchers have developed fluorescein-based probes with customized properties for specific purposes. For example, fluorescein derivatives can be engineered by incorporating specific binding sites to respond to various ions, molecules, or environmental conditions, facilitating the creation of sensors for detecting pH changes, ionic targets, and biological targets. These sensors play a crucial role in environmental monitoring, medical diagnostics, and biochemical research by providing real-time, accurate, and non-invasive measurements of various parameters. The ability to tailor fluorescein probes to specific requirements underscores the compound's versatility and potential for innovation in scientific research and technological advancement. In the past decade, significant progress has been achieved in developing fluorescent probes, due to their interesting photoluminescence behaviour in water. Compared to traditional chromatographic and electrochemical methods, luminescent sensors offer advantages for rapid, highly sensitive, non-destructive, and on-site analysis

Figure 6.1: Some reported Fluorescein derivatives used for metal ion detection.

of specific targets. A large variety of fluorophores encompassing organic molecules, nanomaterials are becoming increasingly available in the literature towards sensor development [6]. A key advantage of synthetic organic molecules is the ability to use chemical techniques to precisely control both the binding functionality and positioning of the fluorophore. Fluorescein is often utilized as the fluorescent core because its distinctive spirolactam structure can exhibit a "turn-on/off" fluorescence response by switching between closed and open forms in certain environments or conditions. This makes it an ideal dye for designing fluorescent probes [7]. The fluorescein-based probes can be tailored through organic synthesis at two key sites: the xanthene ring and the benzoic acid moiety.

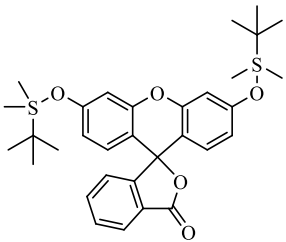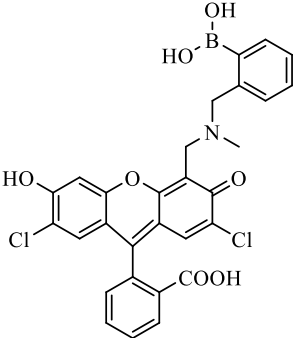| Fluorescein Derivatives	Solvent of study	References
 C6-6	DMSO	[14]
 C6-7	DMSO	[15]
 C6-8	CH₃CN	[16]
 C6-9	HEPES buffer-water	[17]
 C6-10	Tris HCl-CH₃CN	[18]

Fluorescein Derivatives	Solvent of study	References
C6-11	DMF-Water	[19]
C6-12	CH₃CN-MeOH	[20]

Table 6.1: Some reported Fluorescein derivatives used for F⁻ ion binding study.

Therefore, over the past two decades, many advancements have been made in using fluorescein as a sensor probe detecting analytes through fluorescence 'off-on' process [8]. For example, Helal *et al.* demonstrated a fluorescein-imidazole based Schiff base probe which selectively detects Cu^{2+} ions in H_2O/MeOH medium. Upon Cu^{2+} binding, the green fluorescence of the probe quenches due to electron transfer from imidazole to Cu^{2+} [9]. Many fluorescein derivatives incorporating the metal recognition unit in the Spirolactam unit are synthesized and demonstrated them as a fluorescent sensor towards metal ion (Figure 6.1) [9-13]. Similarly, a large number of fluorescein derivatives are also demonstrated as fluoride sensor. The structure and the medium of fluoride detection of some of the fluorescein-based fluoride sensing probes are shown in table 6.1 [14-20].

The literature report revealed that fluorescein alone was not typically used as a probe molecule for sensing cations and anions. Instead, it has been substituted with various functional groups to enhance its sensing capabilities. Additionally, most sensing studies were conducted in organic media rather than pure water, and very few fluorescein derivatives have been mentioned as fluoride ion sensing probes. In this chapter, we have demonstrated the core fluorescein moiety as a fluoride sensor in organic media.

Furthermore, similar to the chapter 5, we have explored the displacement strategy (hypothesis 2) in developing a F⁻ sensing protocol with fluorescein for 100% water medium avoiding any significant interference from other ions.

6.2. Objective of the study

- o To standardised a methodology for the sensing of fluoride ion with Fluorescein dye in 100% water.
- o To study the mechanism of the sensing process.
- o To validate the sensing performance of the methodology with real life sample.

6.3. General experimental details

6.3.1. Synthesis of Fluorescein (M)

Fluorescein was synthesis by standard literature reported method following scheme 6.1.
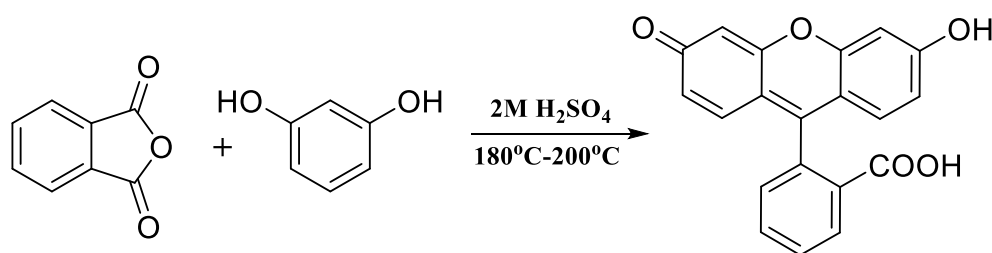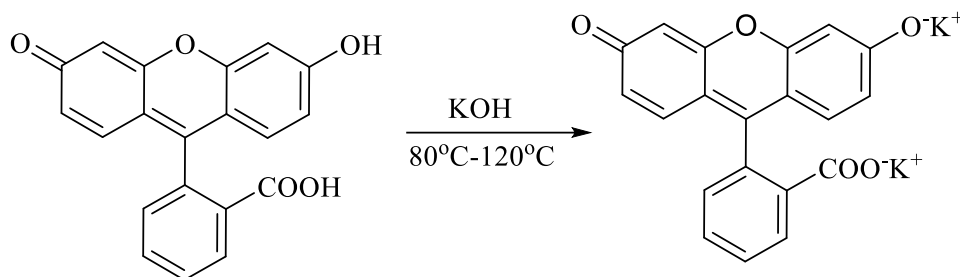

Scheme 6.1: Synthesis of Fluorescein (**M**).

Fluorescein (**M**) was prepared by reacting 0.3 g (2.2 mmol) of phthalic dianhydride with 0.5 g (4.5mmol) of Resorcinol in presence of 6-7 drops of 2M H_2SO_4 in a round bottom flask. Later, the reaction mixture was heated at 180ºC - 200ºC for 30 min and cooled for 5 min after removing it from the reaction bath. After coming to room temperature, 10 mL of acetone was added to the reaction mixture and stirred for another 15-20 min until the solution turns to yellow [21,22].

M: Reddish brown, Yield: 70%, FT-IR of **M** (cm⁻¹): υ(O-H) = 3389.73, υ(C=O) = 1590. ¹H NMR (400 MHz, DMSO-d_6) δ 10.21 (s, 1H), 7.98 (d, J = 7.9 Hz, 1H), 7.85 – 7.64 (m, 1H), 7.26 (d, J = 8.0 Hz, 1H), 6.81 – 6.47 (m, 4H). ¹³C NMR (101 MHz, DMSO-d_6) δ 207.05, 169.25, 160.06, 153.03, 152.38, 136.12, 130.59, 129.55, 126.71, 125.12, 124.58, 113.16, 110.09, 102.79. LCMS (M+H) =333.10 (Calculate: 332.10).

6.3.2. Synthesis of the Potassium salt of fluorescein (K₂M)

Scheme 6.2: Synthesis of Potassium salt of Fluorescein (**K₂M**).

The Potassium salt of fluorescein was synthesized by treating with aqueous KOH (Scheme 6.2). 100 mg of fluorescein was mixed with 100 mg of KOH in 10 mL of water and refluxed overnight. The reaction was stopped and kept idle till precipitated as reddish orange coloured crystal.

K₂M: Reddish orange, Yield: 70%, FT-IR of **M** (cm^{-1}): υ(O-H) = 3442.52, υ(C=O) = 1630.90.

6.3.3. General Procedures for UV−Visible and Fluorescence Spectroscopy Studies

All the sensing experiment of fluorescein (**M**) and potassium salt of fluorescein (**K₂M**) was performed in dimethyl sulphoxide and water solution respectively. The UV-Vis absorption experiments were performed with a 10 μM solution of the probe molecule (**M** in DMSO and **K₂M** in H₂O), while the corresponding fluorescence spectra were recorded with a 1 μM solution at an excitation wavelength of 521 nm at room temperature.

6.3.4. Determination of F⁻ in Water Samples

Different volumes of standard solution of NaF (100 ppm) were added to prepare water samples containing different concentrations of F⁻ required to obtain the calibration plot. The methodology was validated with different concentration of NaF in ppm level prepared in tape water.

6.4. Results and Discussion

6.4.1. F⁻ sensing study of fluorescein (M) in DMSO medium

The anion binding affinity of the **M** was studied by monitoring the change in the UV-Vis spectrum and emission spectra of the probe solution in DMSO upon addition of the tetrabutylammonium salt solution of the anions such as F^-, Cl^-, Br^-, I^-, ClO_4^-, HSO_4^-, $H_2PO_4^-$ and CH_3COO^-. The UV-Vis spectrum of the colourless solution of **M** (10 μM) in DMSO medium showed absorbance at 290 nm. **M** showed affinity towards fluoride and acetate anion, and correspondingly depicts a change in the colour of the solution from colourless to orange. The UV-Vis spectra of **M** solution in DMSO resulted the appearance of a sharp peak at 521 nm upon interaction with F^- and CH_3COO^- ion. Furthermore, **M** showed intense
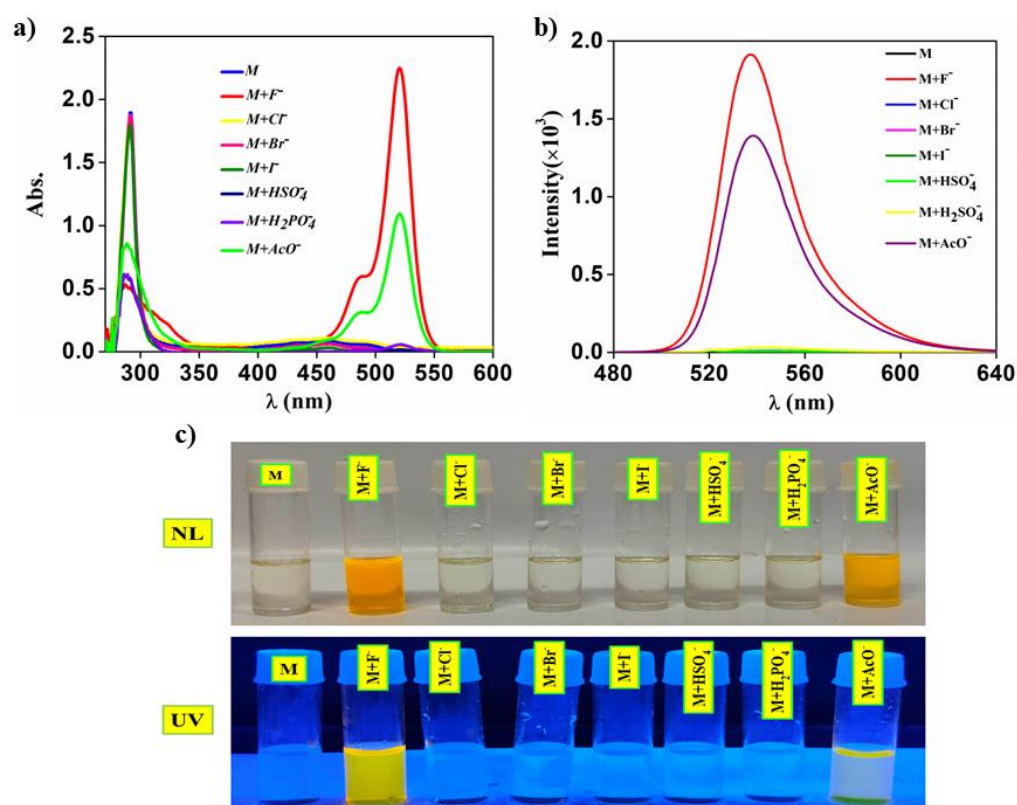

Figure 6.2: (a) UV-Vis spectra of **M** solution (10 μM) in DMSO in presence of different anions (1 x 10⁻² M) as their tetrabutylammonium salt; (b) Emission spectra of **M** solution (1 μM) in DMSO in presence of different anions (1 x 10⁻³ M) as their tetrabutylammonium salt; (c) Colorimetric and fluorometric colour change of the probe molecules in presence of different anions under normal light (NL) and UV-Visible lamp.

fluorescence at 538 nm upon excitation at 521 nm in DMSO solution upon addition of F$^-$ and CH$_3$COO$^-$ ion (figure 6.2). This characteristic optical change might be resulted from the formation of quinonoid structure of fluorescein upon interaction with the strongly basic anions like F$^-$ and CH$_3$COO$^-$ ion. After successfully demonstrating the fluoride affinity of **M** in organic medium, the affinity of the probe molecules towards aqueous fluoride ion was investigated by adding 10 µL of NaF (1 x 10^{-3} M) aqueous solution to the solution of **M** in DMSO. The colour change from colourless to yellowish orange solution was observed, and the absorbance of the peak shifted from 290 nm to 519 nm as observed in case of TBAF **(Figure 6.3a)**. Furthermore, to check the persistency of **M** in presence of water, we performed the dilution experiment by subsequently adding water to **M**.F$^-$ solution in DMSO and observed that upon dilution with H$_2$O, the absorbance of 521 nm peak reduced slightly due to dilution but the colour remains persist (Figure 6.3b).
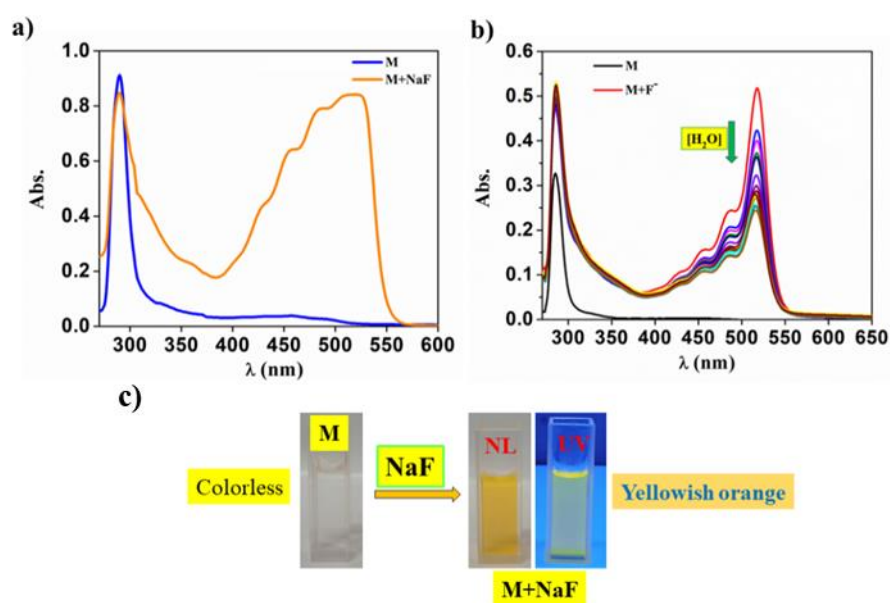

Figure 6.3: UV-Vis spectrum of **(a) M** in DMSO upon addition of 50µL of NaF(1×10^{-2}M) aqueous solution; (b) Change in the UV-Vis spectrum of **M**.NaF solution upon addition of H$_2$O; (c) Change in colour of the solution of **M** upon addition of NaF.

The detection of aqueous F$^-$ by probe **M** provided appreciable results. However, considering the presence of various metal interferents in water, we performed a metal screening experiment. The affinity of the probe molecule towards metal ions were investigated by monitoring both the UV-Vis and fluorescence spectrum of the mixture of **M** in DMSO and aqueous solution of the metal salts (NaCl, MgSO$_4$, VCl$_3$, MnCl$_2$, FeCl$_3$,
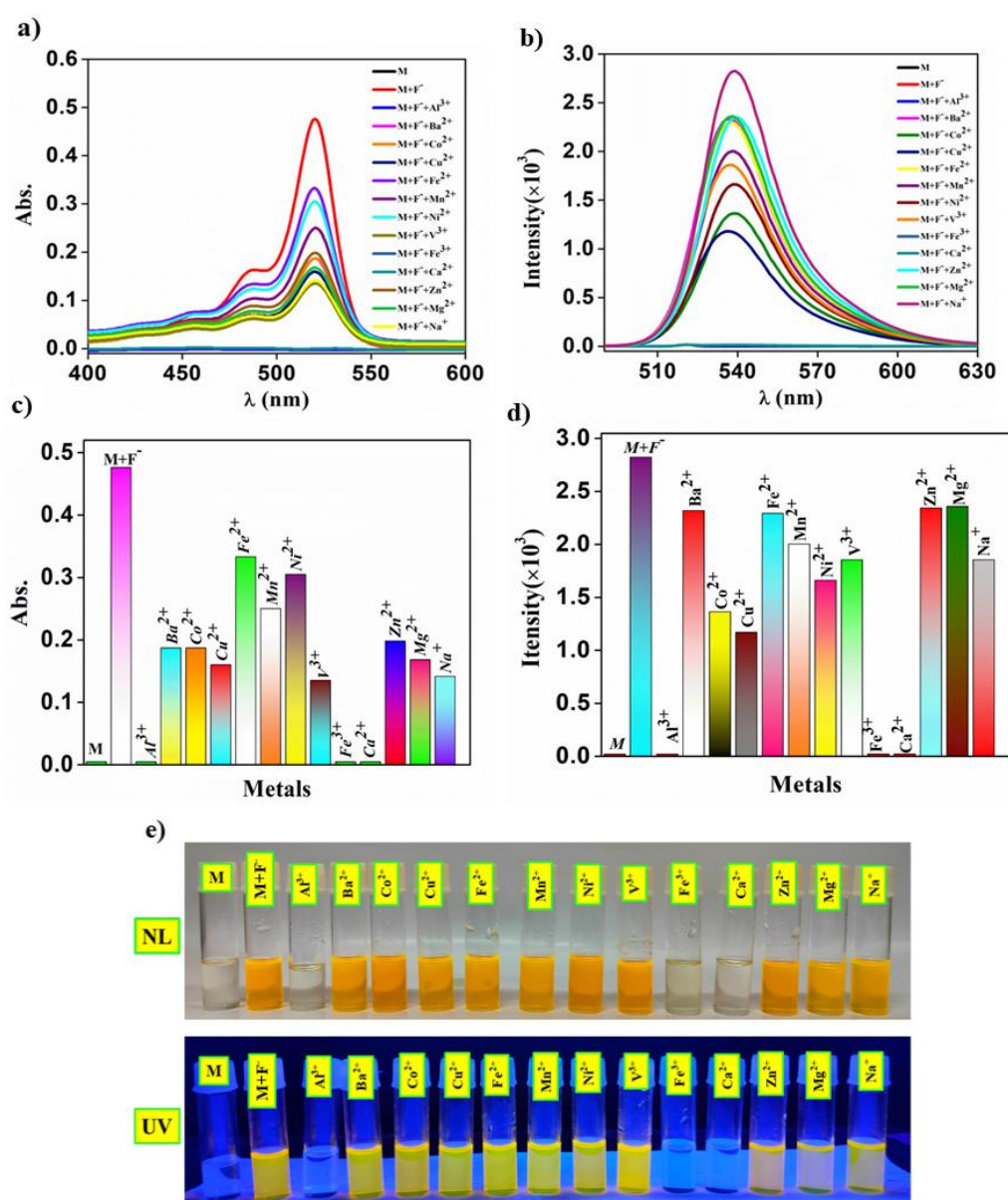
Figure 6.4: (a) UV-Vis spectra of **M** [10 μM] in DMSO solution upon addition of 10 mM aqueous solution of different metal salts (NaCl, MgSO$_4$, VCl$_3$, MnCl$_2$, FeCl$_3$, CoCl$_2$, NiCl$_2$.6H$_2$O, CuCl$_2$.2H$_2$O, ZnCl$_2$, CaCl$_2$, BaSO$_4$, FeCl$_2$, AlCl$_3$) in presence of F$^-$ ion (1 x 10^{-2} M); (b) Emission spectra of **M** [1 μM] in DMSO solution upon addition of 1 mM aqueous solution of different metal salts (NaCl, MgSO$_4$, VCl$_3$, MnCl$_2$, FeCl$_3$, CoCl$_2$, NiCl$_2$.6H$_2$O, CuCl$_2$.2H$_2$O, ZnCl$_2$, CaCl$_2$, BaSO$_4$, FeCl$_2$, AlCl$_3$) in presence of F$^-$ ion (1 x 10^{-2} M); (c) Bar representation of absorbance of the peak at 520nm; (d) Bar representation of emission of the peak at 540 nm (e) Images of colorimetric and fluorometric colour changes.

FeCl$_2$, CoCl$_2$, NiCl$_2$.6H$_2$O, CuCl$_2$.2H$_2$O, ZnCl$_2$, CaCl$_2$, BaSO$_4$ and AlCl$_3$) in presence of F$^-$ ion. It was observed that the probe **M** showed good binding propensity for Al^{3+}, Fe^{3+} and Ca^{2+} ions and the orange colour of the solution disappeared (Figure 6.4). The UV-Vis as well as fluorescence spectra showed the vanishing of the absorption at 521 nm and emission at 537 nm respectively. This observation clearly depicted that the fluoride sensing by probe **M** are likely to be interfered by Al^{3+}, Fe^{3+} and Ca^{2+} ions present in water sample which limits the usefulness of the methodology.

From the metal screening test of **M** in the presence of F$^-$ ion, we observed complete quenching of fluorescence upon adding Al^{3+}, Fe^{3+}, and Ca^{2+}, indicating a fluorescence turn-off response. Clearly, this observation is a crucial prerequisite for our methodology (hypothesis 2). In this regard we are expected to get fluorescence turn-on response from the complexes of **M** with the aforementioned cations as well upon addition of F$^-$ ion. However, on further addition of F$^-$ ion to the quenched solution, the colorimetric and fluorometric signals of **M.F$^-$** solution reappeared in case of Fe^{3+} and Al^{3+} indicating the spontaneous interaction of Al^{3+} and Fe^{3+} with F$^-$ resulting in the formation of $(AlF_x)^{(3-x)+}$ /$(FeF_x)^{(3-x)+}$ complex (Figure 6.5) [23]. This observation prompted us to further explore the use of fluorescein as a optical probe for sensing F$^-$ ions in water, following the concept of hypothesis 2. Consequently, we studied the F$^-$ sensing affinity of the K-salt of fluorescein (**K$_2$M**).
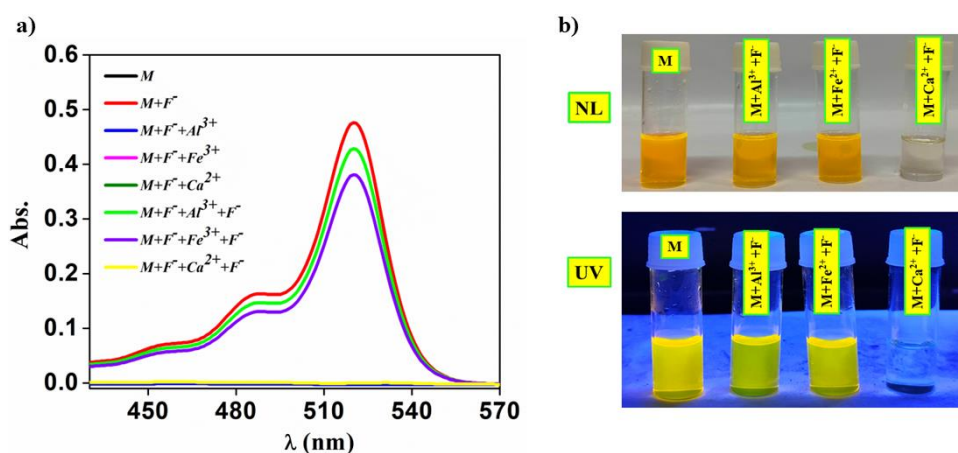

Figure 6.5: (a) UV-Vis spectra of **M**-metal complex upon re-addition of aqueous NaF (1 × 10^{-2} M) in presence of metal like Ca^{2+}, Fe^{3+} and Al^{3+}; (b) Images of the corresponding colorimetric and fluorometric colour change.

6.4.2. F⁻ sensing study of potassium salt of fluorescein (K₂M) in water medium

Due to the good solubility and optical properties of **K₂M** in water, the F⁻ sensing experiment was performed in aqueous solution. As depicted in Figure 6.6, aqueous solution of **K₂M**
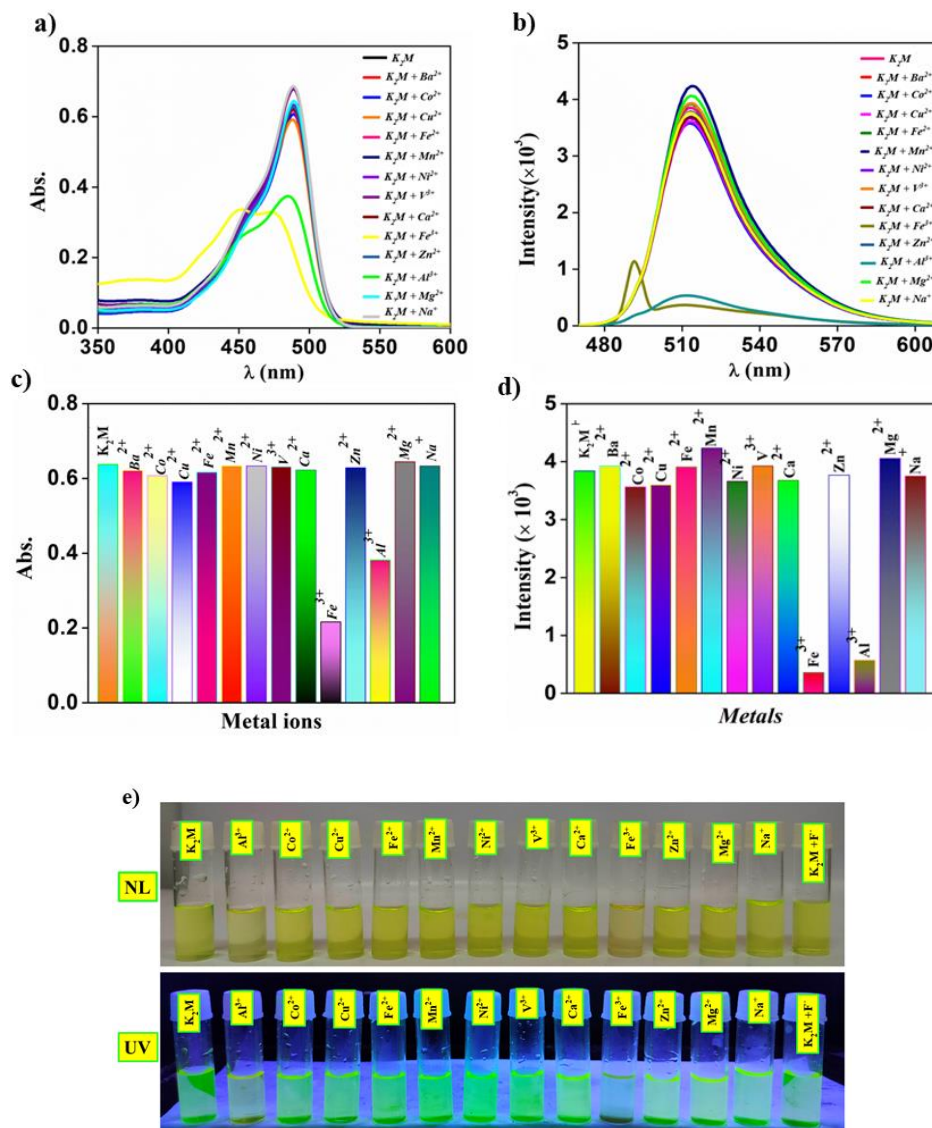

Figure 6.6: (a) UV-Vis spectra of **K₂M** [10 μM] in water solution upon addition of 10 mM aqueous solution of different metal salts (NaCl, MgSO₄, VCl₃, MnCl₂, FeCl₃, CoCl₂, NiCl₂.6H₂O, CuCl₂.2H₂O, ZnCl₂, CaCl₂, BaSO₄, FeCl₂, AlCl₃) in presence of F⁻ ion; (b) Emission spectra of **K₂M** [1 μM] in water solution upon addition of 1 mM aqueous solution of different metal salts (NaCl, MgSO₄, VCl₃, MnCl₂, FeCl₃, CoCl₂, NiCl₂.6H₂O, CuCl₂.2H₂O, ZnCl₂, CaCl₂, BaSO₄, FeCl₂, AlCl₃) in presence of F⁻ ion; (c,d) Bar representation of above two titrations; (e) Images of the colorimetric and fluorometric colour change (NL: Normal light, UV: UV light).

solution in water showed absorption peaks at around 490 nm. **K₂M** displayed emission peak at $\lambda_{em} = 513$ nm upon excitation excitation with $\lambda_{exc} = 490$ nm radiation. On addition of Al^{3+} (aq) solution to the **K₂M** solution in water, there is a noticeable colour change of the solution from greenish yellow to pale reddish yellow. UV-Vis titration experiments revealed the lowering of the intensity of absorption peak at 490 nm of **K₂M** solution with concomitant evolution of a broad peak at 453- 487 nm, which become saturated after adding 80μL of 10mM Al^{3+} aqueous solution (Figure 6.7a). Subsequently, fluorescence measurement also revealed the gradual fluorescence quenching of **K₂M** solution in presence of Al^{3+} ion and complete quenching of fluorescence was observed once the concentration of Al^{3+} reaches 0.026 mM (Figure 6.7b). These findings attributed to the binding of Al^{3+} with the fluorescein leading to the formation of an *in-situ* Al^{3+}-fluorescein
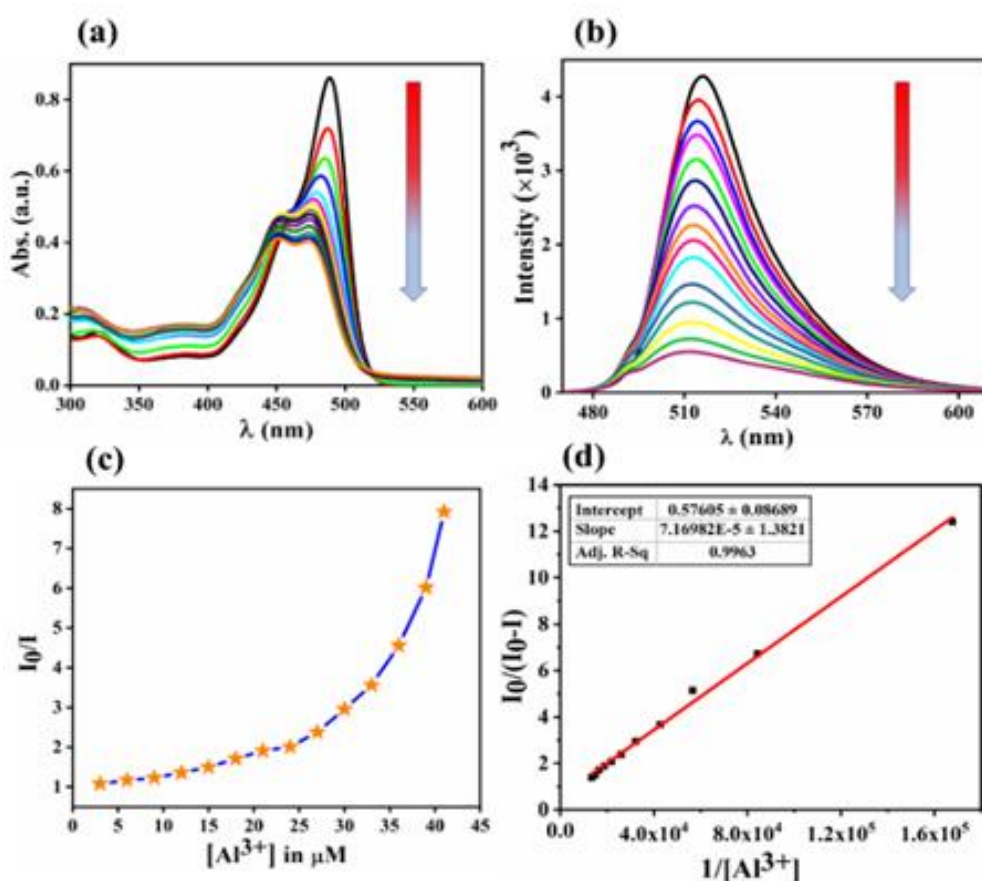

Figure 6.7: (a) UV-Vis spectra of **K₂M** solution in water upon gradual addition of Al^{3+} ion; (b) Emission spectra of **K₂M** solution in water upon gradual addition of Al^{3+} ion; (c) Stern-Volmer plot of quenching of emission of **K₂M** solution upon addition of Al^{3+}; (d) Benesi-Hildebrand plot of the fluorescence titration data.
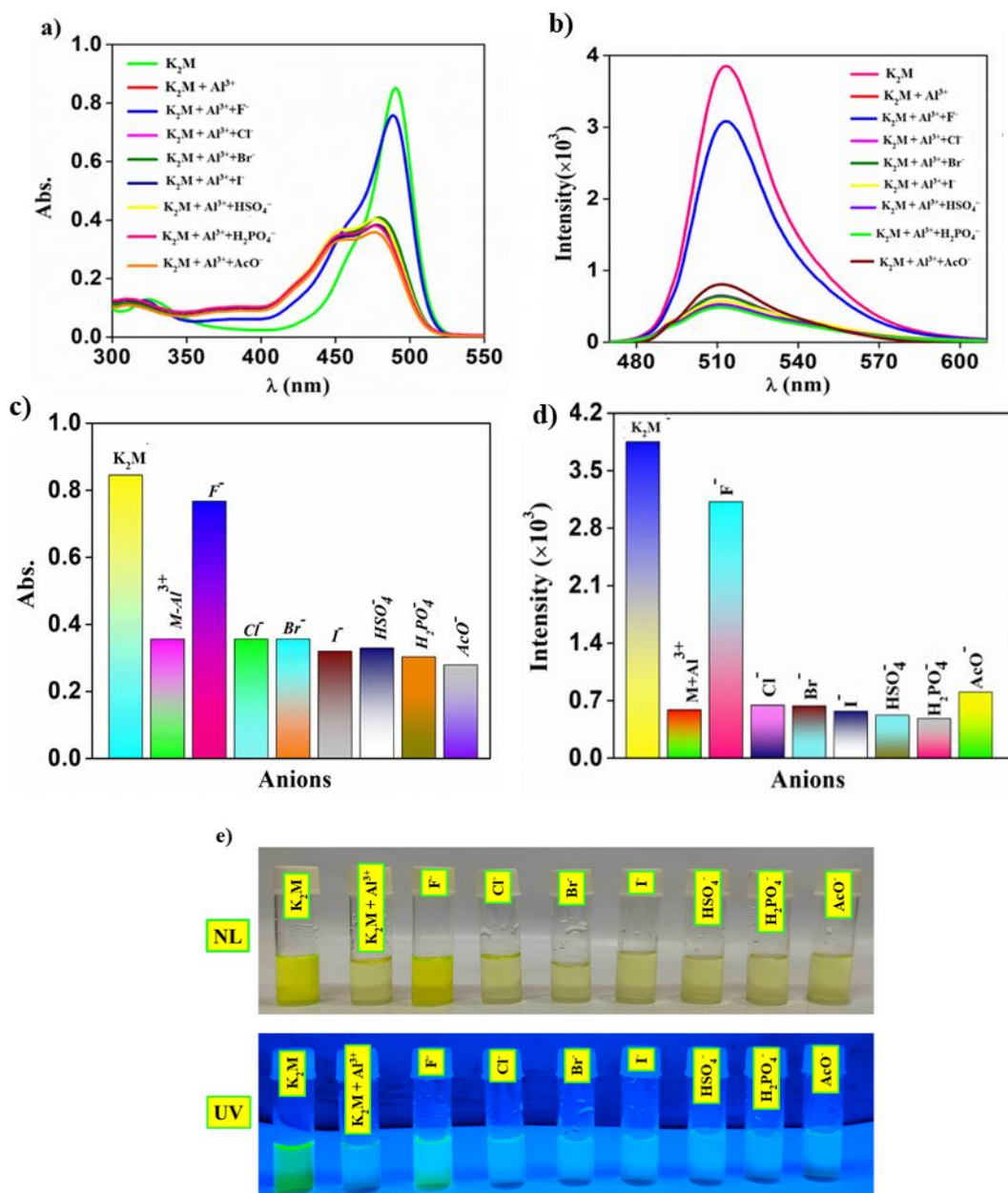
Figure 6.8: (a) UV-Vis spectra of probe **K₂M** (10 µM) in water upon addition of different anions (1 x 10⁻² M)in presence of Al³⁺ (1 x 10⁻² M); (b) Emission spectra of probe **K₂M** (1 µM) in water upon addition of different anions (1 x 10⁻³ M)in presence of Al³⁺ (1 x 10⁻³ M); (c) Bar representation of the change in absorbance; (d) Bar representation of the change of emission intensity; (e) Image of colorimetric and fluorometric changes.

complex. The plot of $\frac{I_0}{I}$ vs [Al³⁺] plot showed exponential increase upon addition of Al³⁺ ion revealing the static nature of quenching of fluorescence of **K₂M** indicating ground state

complexation (figure 6.7c) [24]. From the plot of $\frac{I_0}{I_0 - I}$ vs $\frac{1}{[Al^{3+}]}$, the equilibrium constant for the complexation reaction (considering the linear variation up to 27 µM addition of F⁻) was calculated and found as 8.03×10^3 M⁻¹ [25]. After the successful observation of complete quenching of **K₂M** by the addition of Al³⁺ ion, we investigated the affinity Al³⁺-**K₂M** mixture in water towards the various anions. The UV-Vis titration study of different anions revealed that the absorption peaks at 490 nm reappears only upon addition of F⁻ ion with the fluorescence turn-on response, whereas other anions failed to do so (Figure 6.8). This observation suggested that F⁻ ion has taken way the Al³⁺ from the Al³⁺-fluorescein complex forming the stable $(AlF_x)^{(3-x)+}$ complex and the colour changes from brownish red to greenish yellow as the original **M²⁻** reappeared in the reaction mixture. UV-Vis titration study revealed that upon incremental addition of NaF, the broad peaks at 453-487 nm disappeared with simultaneous increase in the intensity of the peak at 490 nm (Figure 6.9a).
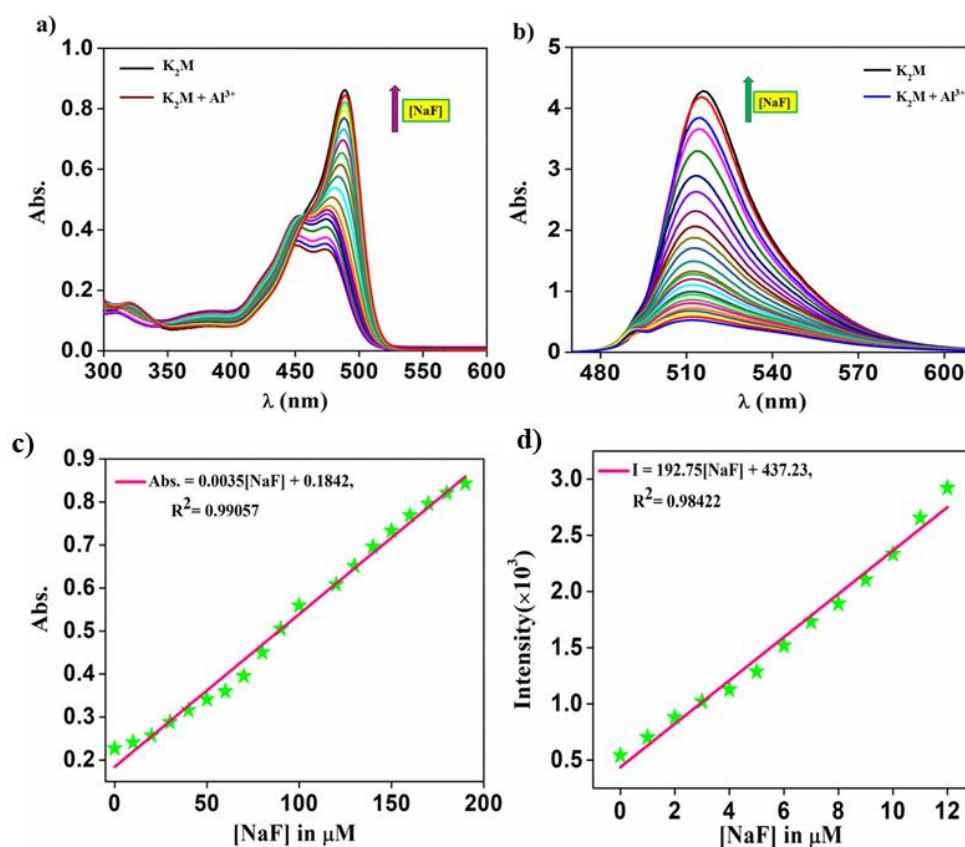

Figure 6.9: (a) UV-Vis absorption spectra of **K₂M**-Al³⁺ solution upon gradual addition of F⁻ in water medium; (b) Emission spectra of **K₂M**-Al³⁺ upon gradual addition of F⁻ in water medium; (c) plot of the change in absorbance vs [NaF]; d) plot of the change in intensity of emission vs [NaF].
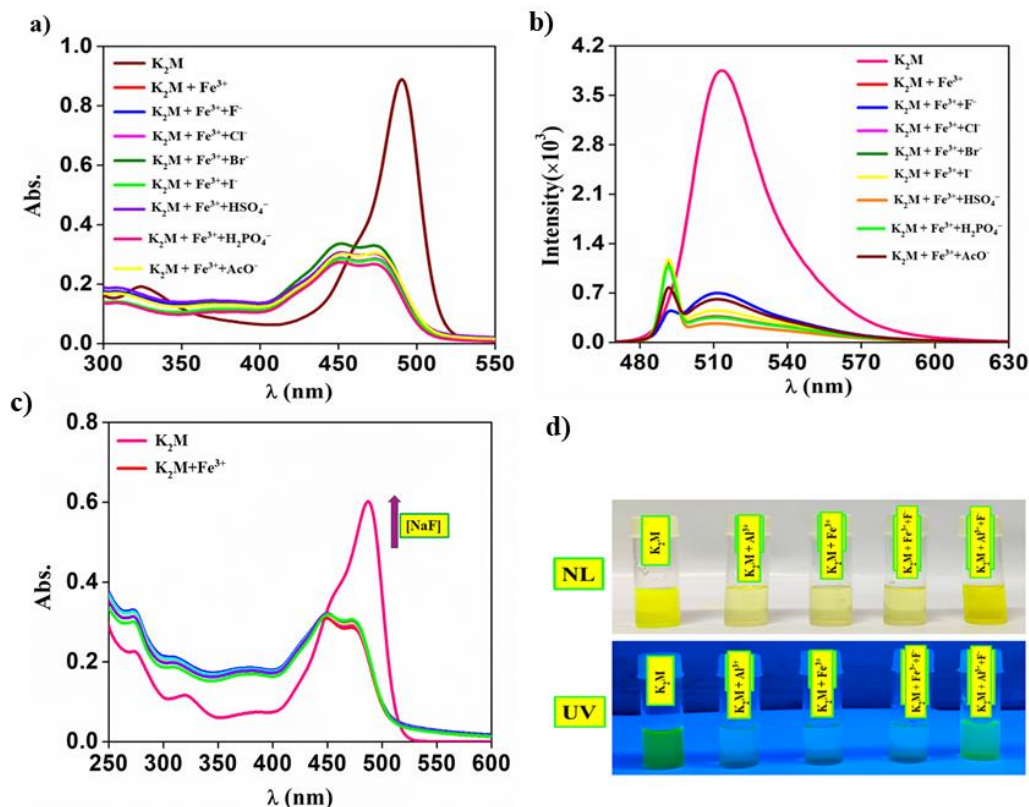
Figure 6.10: (a) UV-Vis absorption spectra of **K₂M**-Fe³⁺ solution upon addition of different anions in water medium; (b) Emission spectra of **K₂M**-Fe³⁺ upon addition of different anions in water medium; (a) UV-Vis absorption spectra of **K₂M**-Fe³⁺ solution upon gradual addition of F⁻ in water medium; (d) Images of colorimetric and fluorometric changes.

Additionally, the fluorescence titration study also revealed the gradual recurrence of emission spectra of the **K₂M** solution upon incremental addition of NaF solution (Figure 6.9b). Interestingly, the consecutive addition of NaF to the solution of **K₂M** whose emission has been quenched by Fe³⁺ ion showed no sign of recurrence of yellowish green fluorescence colour even after the concentration of NaF has been increased. This observation conferred that **K₂M** molecule excludes the possibility of interference from the other tested ions during F⁻ recognition and emphasized the highly selective response of the methodology for F⁻ (Figure 6.10).

To study the sensitivity of F⁻ ion recognition by the in situ formed Al³⁺-fluorescein complex, increasing concentrations of F⁻ (aq) in ppm level were introduced into the solution of the mixture of **K₂M** and Al³⁺ complex in water (Figure 6.11). The emission plot clearly portrayed the fluorescence turn-on phenomenon, maintaining a linear relationship between the intensity of the respective optical changes with the increasing concentration of

NaF. The absorbance data showed a good linear relationship within the range of 0 to 10 ppm (0 to 526 µM) with a LOD value of 0.3 ppm ($R^2 = 0.98$) (Figure 6.11 a,c). Furthermore, the intensity of 515 nm emission increased linearly with the increase in concentration of F^- (Figure 6.11 b,d) within the range of 0 to 10 ppm (0 to 526 µM). The LOD calculated from the fluorescence intensity curve was found to be 2 ppb ($R^2 = 0.98$), which is lower than that calculated from the absorbance value. The low LOD values implied that the bifunctional (colorimetric and fluorescence) sensing approach for F^- in a water medium with K_2M salt is more suitable for practical application than that of M.
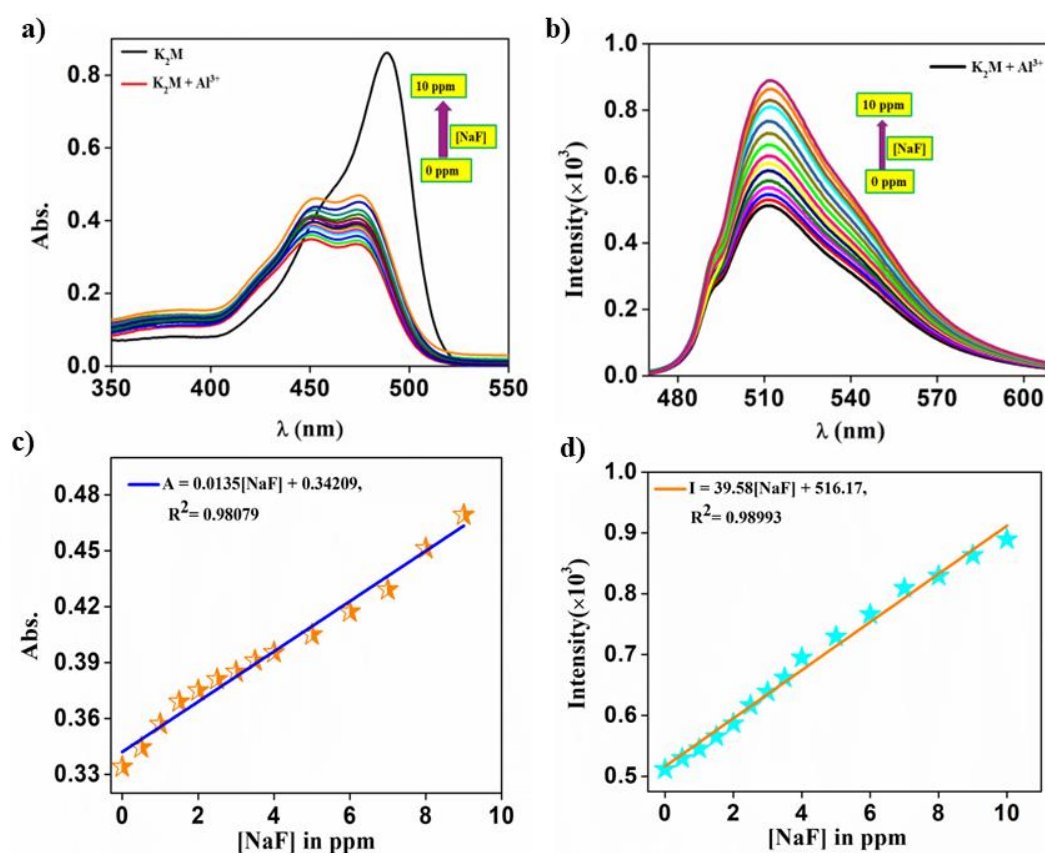

Figure 6.11: (a) UV-Vis absorption spectra of K_2M-Al^{3+} solution upon gradual addition of F^- in ppm level in water medium; (b) Emission spectra of K_2M-Al^{3+} upon gradual addition of F^- in ppm level in water medium; (c) change in absorbance vs [NaF]; (d) change in emission intensity vs [NaF].

Quantum yield calculations also showed that upon the sequential addition of Al^{3+} (1 mM) and NaF (1 mM) to K_2M solution, the quantum yield drops from 92% (with an average lifetime of 26.72 ns) to 13% resulting in an average lifetime of 22.81 ns. Notably, the subsequent addition of an excess of F^- to the K_2M solution in the presence of Al^{3+} leads to

fluorescence turn-on, with the quantum yield regaining 90% (with an average lifetime of 25.93 ns). Thus, this observation revealed that the dye, fluorescein, could be a high-contrast dual optical sensor when used as its potassium salt. (Figure 6.12). The similar life time of **K₂M** in presence in absence of quencher Al^{3+}also supported the static quenching of the fluorescence of **K₂M** by Al^{3+}.
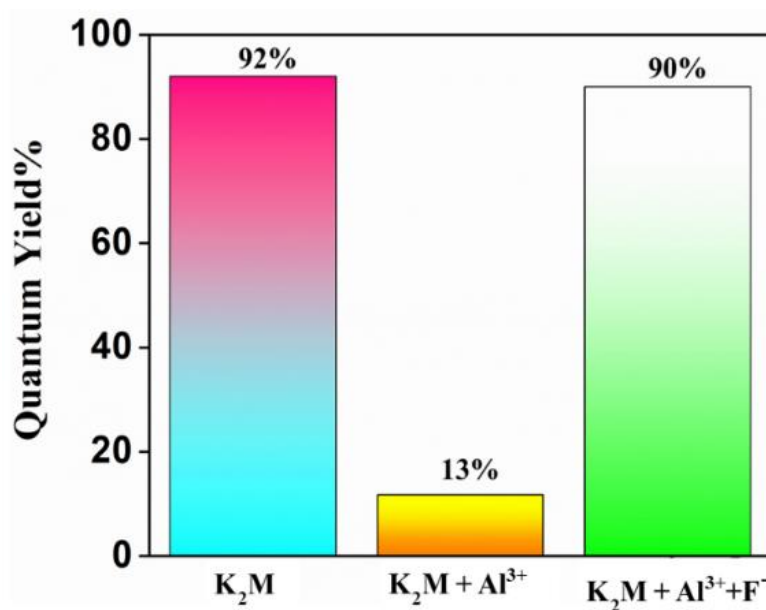

Figure 6.12: Change in the quantum yield of **K₂M** upon sequential addition of Al^{3+} and NaF in water.

6.4.3. Recyclability study

To test the reversibility of the sensing process, Al^{3+} was added to the solution, and the absorbance and emission behaviour of the solution containing all three components (**K₂M**, AlCl₃, and NaF) were monitored. The study revealed the emergence of a broad UV-Vis absorption peak at 455-480 nm as well as the quenching of the emission at 490 nm upon addition Al^{3+} solution. Subsequent addition of F^- ions led to the diminished absorption at 455-480 nm and simultaneously the fluorescence emission at 515 nm was turned on. With the alternating addition of F^- and Al^{3+}, the switching of absorbance and fluorescence could be recycled for at least four times (Figure 6.13), indicating good recyclability of the sensor in this methodology.
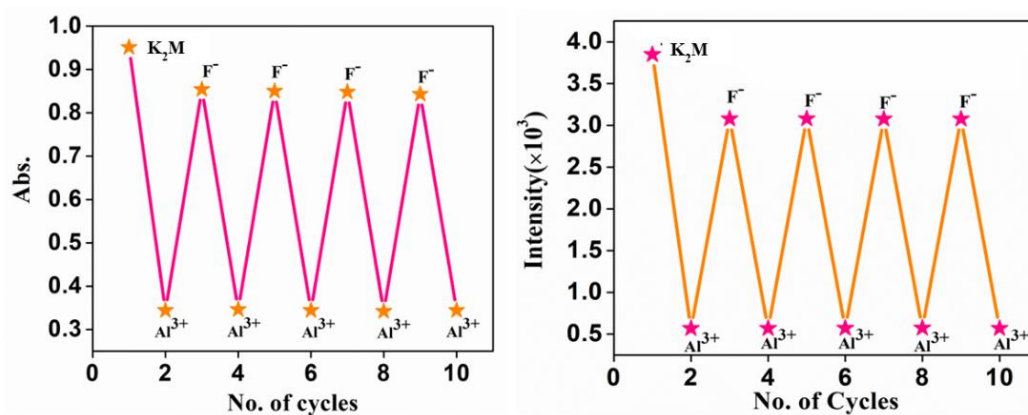
Figure 6.13: Recyclability of the probe studied by (a) UV−vis absorption spectroscopy and (b) fluorescence spectra.

6.4.4. Investigation of the sensing mechanism

Al^{3+} (aq) is known as a hard metal ion, and it forms stable complexes with strong hard bases like the F^- ion [26,27]. Compared to F^-, oxygens are relatively less hard, so F^- can easily
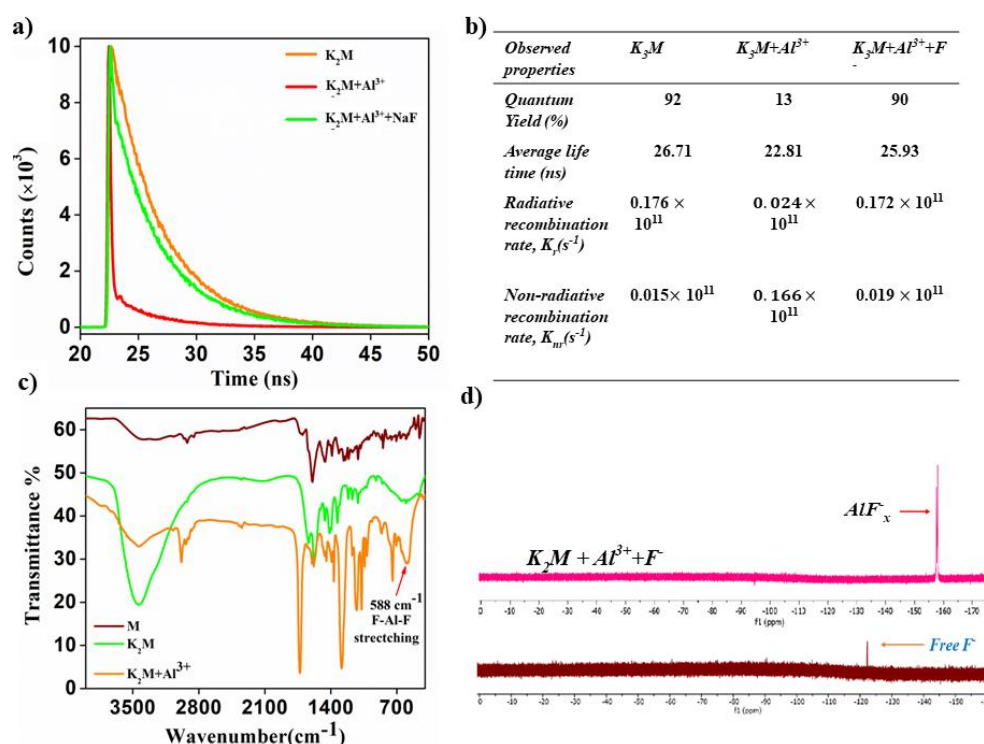

Figure 6.14: (a) Time resolved photoluminescence spectra of **K₂M** in presence of Al^{3+} and F^-; (b) characteristic photophysical parameters; (c) FTIR spectra of **K₂M** and **K₂M** in presence of Al^{3+} and F^-; (d) ^{19}F NMR spectra: top- **K₂M**, Al^{3+} and F^- mixture in D_2O; bottom: **K₂M** and F^- mixture in D_2O.
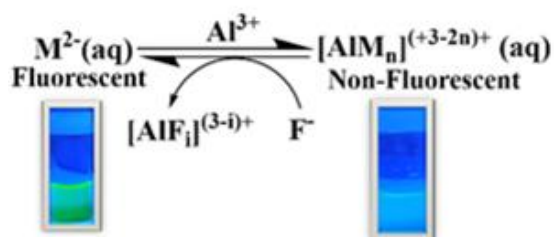
Figure 6.15: Plausible pathway of the sensing process.

bind with Al^{3+} to form a complex with a fluorescein ligand, resulting in a stable $(AlF_i)^{(3-i)+}$(aq) complex [28]. Notably, the average lifetime of **K₂M** does not changes appreciably upon addition of ions (Al^{3+} and F^-) indicating static quenching behaviour, implying all the ion exchange occurs in the ground state of fluorescein [24,29]. Further addition of F^-, results in fluorescence turns on phenomenon, suggesting the removal of Al^{3+} ions by F^- due to the formation of Al-fluoride complexes which eventually led to the release of the dye. FT-IR analysis confirmed the formation of the $(AlF_x)^{(3-x)+}$ complex, revealing a peak at 588 cm^{-1} attributed to the vibrational stretching of F-Al-F (Figure 6.15c) [30]. Further confirmation was provided by ^{19}F-NMR (D₂O as the solvent), showing a peak at -159 ppm, which also indicated the formation of AlF_x^- species in the solution (Figure 6.15d) [31]. These findings clearly pointed out the F^- ion induced decomplexation of Al^{3+}-fluorescein complex due to strong HSAB interaction between Al^{3+} and F^- ion (Figure 6.16).

6.5. Validation of the method with real life sample

To check the applicability of the methodology towards detection of NaF in water, we have checked our methodology's performance with laboratory prepared samples having different ppm level concentrations of F^-. For the UV-Vis analysis, 3 mL of a 10 μM M solution of **K₂M** was placed in a cuvette, and 80 μL aqueous solution of 1×10^{-2} M AlCl₃ in an aqueous medium was added. Subsequently, 50 μL of each water sample was added separately to each mixture. Similarly, for fluorescence measurement, 3 mL of 1 μM solution of **K₂M** was placed in a cuvette, and 80 μL of a 1×10^{-3} M AlCl₃ solution in an aqueous medium was added. Then, 50 μL of each water sample was added separately to each mixture. The data was then compared with the calibration plot to determine the concentration of fluoride ions in the water samples. The water samples exhibited a significant fluorometric change, transitioning from pale yellowish-red to greenish-yellow, indicative of fluoride ion's presence (Figure 6.16 a-c). The fluoride ion concentration was determined from the
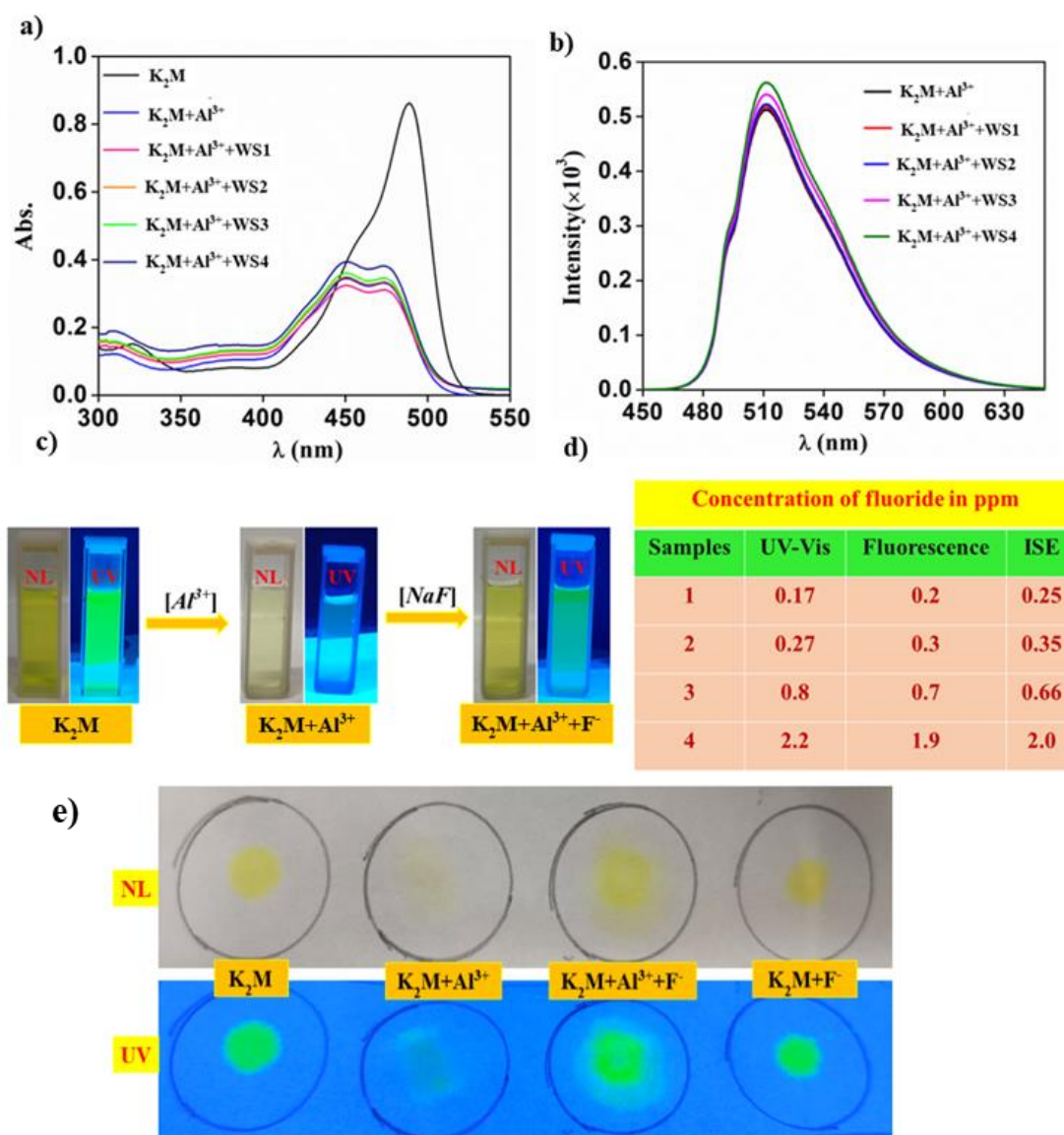
Figure 6.16: Measurement of the concentration of fluoride in the water sample (a) UV-Vis spectra, (b) emission spectra, (c) change in colour of the solution upon addition of water sample; (d) comparison of the fluoride data estimated with our methodology with ion selective electrode (ISE) data; (e) Cellulose paper strip test.

calibration curve. These results were in good agreement with those obtained from ion selective electrode (ISE) measurements, (Figure 6.16d). This observation underscores the capability of our methodology to both qualitatively and quantitatively assess the presence of fluoride ions in aqueous media. Furthermore, the applicability of the methodology is also tested in cellulose paper strip as mentioned in chapter 5 and found that the methodology can be used in the paper strip too with good recyclability of the strip (Figure 6.16e).

6.6. Conclusion

The potassium salt of fluorescein (**K₂M**) is demonstrated as a fluorometric as well as colorimetric probe for recognition of F^- ion in water medium. **K₂M** showed turn off fluorescence response in presence of Al^{3+} ions. However, subsequent addition of fluoridated water potrayed naked eye discernible fluorescence turns on response. The LOD value calculated for F^- ion is found to be 0.3 ppm and 2 ppb for UV-Vis and Fluorometric technique respectively. The detection range is found to be within the concentration limit set by WHO for fluoride ion in drinking water. This method showed some minor interference from Fe^{3+} ion. The present work highlights a method for rapid and sensitive detection of F^- ion in 100 % water medium with high precision with the aid of a common organic fluorescent dye, fluorescein.

6.7. References

[1]   Nagendrappa, G. Johann Friedrich Wilhelm Adolf von Baeyer: A pioneer of synthetic organic chemistry. *Resonance*, 19:489-522, 2014.

[2]   Duan, Y., Liu, M., Sun, W., Wang, M., Liu, S., and Li, Q. X. Recent progress on synthesis of fluorescein probes. *Mini-Reviews in Organic Chemistry*, 6(1):35-43, 2009.

[3]   Moore, G. E., Peyton, W. T., French, L. A., and Walker, W. W. The clinical use of fluorescein in neurosurgery: the localization of brain tumors. *Journal of neurosurgery*, 5(4):392-398, 1948.

[4]   Sjöback, R., Nygren, J., and Kubista, M. Absorption and fluorescence properties of fluorescein. *Spectrochimica Acta Part A: Molecular and Biomolecular Spectroscopy*, 51(6):L7-L21, 1995.

[5]   Brannon, J. H., and Magde, D. Absolute quantum yield determination by thermal blooming. Fluorescein. *The Journal of Physical Chemistry*, 82(6):705-709, 1978.

[6]   Yin, W., Zhu, H., and Wang, R. A sensitive and selective fluorescence probe-based fluorescein for detection of hypochlorous acid and its application for biological imaging. *Dyes and Pigments*, 107:127-132, 2014.

[7]   Wang, D., Xiang, X., Yang, X., Wang, X., Guo, Y., Liu, W., and Qin, W. Fluorescein-based chromo-fluorescent probe for zinc in aqueous solution: Spirolactam ring opened or closed?. *Sensors and Actuators B: Chemical*, 201:246-254, 2014.

[8]   Li, T., Yang, Z., Li, Y., Liu, Z., Qi, G., and Wang, B. A novel fluorescein derivative as a colorimetric chemosensor for detecting copper (II) ion. *Dyes and Pigments*, 88(1):103-108, 2011.

[9]   Helal, A., Kim, H. S., Yamani, Z. H., and Nasiruzzaman Shaikh, M. Fluorescein-N-methylimidazole conjugate as Cu^{2+} sensor in mixed aqueous media through electron transfer. *Journal of fluorescence*, 26:1-9, 2016.

[10] Piyanuch, P., Watpathomsub, S., Lee, V. S., Nienaber, H. A., and Wanichacheva, N. Highly sensitive and selective Hg^{2+}-chemosensor based on dithia-cyclic fluorescein for optical and visual-eye detections in aqueous buffer solution. *Sensors and Actuators B: Chemical*, 224:201-208, 2016.

[11] Fan, C., Luo, S., and Liu, R. Optimization of an analytical method for the spectrophotometric determination of copper in tea and water samples after ultrasonic assisted cloud point extraction using a benzothiazole fluorescein derivative complexing agent. *RSC advances*, 5(80):65321-65327, 2015.

[12] Chantalakana, K., Choengchan, N., Yingyuad, P., and Thongyoo, P. A highly selective 'turn-on'fluorescent sensor for Zn^{2+} based on fluorescein conjugates. *Tetrahedron Letters*, 57(10):1146-1149, 2016.

[13] Lee, M. H., Wu, J. S., Lee, J. W., Jung, J. H., and Kim, J. S. Highly sensitive and selective chemosensor for Hg^{2+} based on the rhodamine fluorophore. *Organic Letters*, 9(13):2501-2504, 2007.

[14] Zhang, X., Shiraishi, Y., and Hirai, T. Unmodified fluorescein as a fluorescent chemosensor for fluoride ion detection. *Tetrahedron Letters*, 48(50):8803-8806, 2007.

[15] Kim, H. Y., Im, H. G., and Chang, S. K. Colorimetric and fluorogenic signaling of fluoride ions by thiophosphinated dichlorofluorescein. *Dyes and Pigments*, 112:170-175, 2015.

[16] Asthana, S. K., Kumar, A., and Upadhyay, K. K. A reaction based chromofluorogenic turn-on probe for specific detection of fluoride over sulfide/thiols. *Tetrahedron Letters*, 55(43):5988-5992, 2014.

[17] Zheng, F., Zeng, F., Yu, C., Hou, X., and Wu, S. A PEGylated Fluorescent Turn-On Sensor for Detecting Fluoride Ions in Totally Aqueous Media and Its Imaging in Live Cells. *Chemistry–A European Journal*, 19(3):936-942, 2013.

[18] Chereddy, N. R., Nagaraju, P., Raju, M. N., Saranraj, K., Thennarasu, S., and Rao, V. J. A two fluorophore embedded probe for collective and ratiometric detection of Hg^{2+} and F^- ions. *Dyes and Pigments*, 112:201-209, 2015.

[19] Yang, X. F., Ye, S. J., Bai, Q., and Wang, X. Q. A fluorescein-based fluorogenic probe for fluoride ion based on the fluoride-induced cleavage of tert-butyldimethylsilyl ether. *Journal of fluorescence*, 17:81-87, 2007.

[20] Swamy, K. M. K., Lee, Y. J., Lee, H. N., Chun, J., Kim, Y., Kim, S. J., and Yoon, J. A new fluorescein derivative bearing a boronic acid group as a fluorescent chemosensor for fluoride ion. *The Journal of Organic Chemistry*, 71(22):8626-8628, 2006.

[21] Sun, W. C., Gee, K. R., Klaubert, D. H., and Haugland, R. P. Synthesis of fluorinated fluoresceins. *The Journal of Organic Chemistry*, 62(19):6469-6475, 1997.

[22] Tremayne, M., Kariuki, B. M., and Harris, K. D. Structure Determination of a Complex Organic Solid from X-Ray Powder Diffraction Data by a Generalized Monte Carlo Method: The Crystal Structure of Red Fluorescein. *Angewandte Chemie International Edition in English*, 36(7):770-772, 1997.

[23] King, E. L., and Gallagher, P. K. The Thermodynamics of Aluminum (III) Fluoride Complex Ion Reactions. The Graphical Evaluation of Equilibrium Quotients from n ([X]). *The Journal of Physical Chemistry*, 63(7):1073-1076, 1959.

[24] Baranowski, M., Urban, J. M., Zhang, N., Surrente, A., Maude, D. K., Andaji-Garmaroudi, Z., and Plochocka, P. Static and dynamic disorder in triple-cation hybrid perovskites. *The Journal of Physical Chemistry C*, 122(30):17473-17480, 2018.

[25] Van de Weert, M., and Stella, L. Fluorescence quenching and ligand binding: A critical discussion of a popular methodology. *Journal of Molecular Structure*, 998(1-3):144-150, 2011.

[26] Pearson, R. G. Hard and soft acids and bases. *Journal of the American Chemical society*, 85(22):3533-3539, 1963.

[27] Pearson, R. G., and Songstad, J. Application of the principle of hard and soft acids and bases to organic chemistry. *Journal of the American Chemical Society*, 89(8):1827-1836, 1967.

[28] Bond, A. M., and Hefter, G. T. *Critical survey of stability constants and related thermodynamic data of fluoride complexes in aqueous solution* (No. 27). Elsevier, 2017.

[29] Pal, A., Srivastava, S., Saini, P., Raina, S., Ingole, P. P., Gupta, R., and Sapra, S. Probing the mechanism of fluorescence quenching of QDs by Co (III)-Complexes: size of QD and nature of the complex both dictate energy and electron transfer processes. *The Journal of Physical Chemistry C*, 119(39):22690-22699, 2015.

[30] König, R., Scholz, G., Scheurell, K., Heidemann, D., Buchem, I., Unger, W. E. S., and Kemnitz, E. Spectroscopic characterization of crystalline AlF_3 phases. *Journal of fluorine chemistry*, 131(1):91-97, 2010.

[31] Jin, Y., Molt Jr, R. W., Pellegrini, E., Cliff, M. J., Bowler, M. W., Richards, N. G., and Waltho, J. P. Assessing the Influence of Mutation on GTPase Transition States by Using X-ray Crystallography, ^{19}F NMR, and DFT Approaches. *Angewandte Chemie International Edition*, 56(33):9732-9735, 2017.